Low-energy electron diffraction from quasicrystal surfaces

2003 J. Phys.: Condens. Matter 15 R63

(http://iopscience.iop.org/0953-8984/15/3/201)

INSTITUTE OF PHYSICS PUBLISHING JOURNAL OF PHYSICS: CONDENSED MATTER

J. Phys.: Condens. Matter **15** (2003) R63–R81 PII: S0953-8984(03)39405-6

TOPICAL REVIEW

Low-energy electron diffraction from quasicrystal surfaces

R D Diehl[1], J Ledieu[2], N Ferralis[1], A W Szmodis[1] and R McGrath[2]

[1] Physics Department and Materials Research Institute, Penn State University, University Park, PA 16802, USA
[2] Department of Physics and Surface Science Research Centre, University of Liverpool, Liverpool L69 3BX, UK

Received 2 October 2002
Published 13 January 2003
Online at stacks.iop.org/JPhysCM/15/R63

Abstract

The discovery of ordered but aperiodic quasicrystal structures has required the development of new diffraction methods to determine their structures. The purpose of this review is to highlight the challenges posed by the aperiodicity of quasicrystals to the study of their surface structures by low-energy electron diffraction (LEED). This paper describes how the LEED technique has been thus far adapted to study several quasiperiodic surface structures, and summarizes the results of those studies. It also presents new spot-profile-analysis LEED results from the fivefold surface of Al–Pd–Mn. An x-ray diffraction experiment and a He-atom diffraction experiment, both on Al–Pd–Mn, are also described for comparison.

Contents

1. Introduction

Quasicrystals form a class of materials discovered in 1982 that are well ordered, but aperiodic. So far, all known quasicrystalline materials are alloys, and hundreds of quasicrystals have been identified. Quasicrystal structures have no periodically repeating 'unit cell'. The type of order present in a quasicrystal is exemplified by the two-dimensional tilings developed by Penrose (see figure 1) and others, and discussed in a recent review in this journal [1]. These structures produce well defined diffraction patterns that differ from 'conventional' diffraction patterns by the presence of axes of five- and tenfold rotational symmetry, and by the aperiodic spacing between diffraction peaks. To include quasicrystalline structures in the definition of a crystal, the International Union of Crystallography revised its definition to include any solid with 'an essentially discrete diffraction pattern' [2].

Diffraction has been the predominant experimental technique for determining the structures of ordered materials for nearly a century. For the past 30 years, it has also been the primary method used for the quantitative determination of surface structures [3]. The symmetry and periodicity inherent in crystalline structures historically have provided the fundamental underpinnings of the theory of diffraction. So when the definition of a crystal was broadened in 1992 to include aperiodic structures with previously disallowed symmetries, such as five- and tenfold rotational invariance, the diffraction community was challenged to reformulate the conventional methods to incorporate the resulting broader range of possible crystalline structures.

Low-energy electron diffraction (LEED) is the technique used most often for the determination of surface geometries [3]. This review provides a brief description of the LEED technique as applied to periodic structures. This is followed by a description of the new challenges posed by quasicrystal surfaces to the determination of surface geometries using LEED, and a description of the new approaches that have been employed to meet these challenges. The most important structural studies to date of quasicrystal surfaces using LEED are presented and discussed. Finally, two studies using other diffraction techniques to study quasicrystals are briefly described for comparison.

2. Low-energy electron diffraction from periodic crystals

2.1. The LEED experiment

A typical geometry for a LEED experiment is shown in figure 2. The reason that LEED is such a common technique in surface science laboratories is that it is relatively inexpensive, compact and simple to perform in an ultra-high vacuum chamber used for surface science experiments. The typical LEED optics consists of a filament that provides a nearly monoenergetic source of electrons by thermionic emission, focusing electrodes that are used to produce a narrow beam of electrons and a detector assembly that usually includes a set of grids used for eliminating the inelastically scattered electrons and a phosphor screen. Data can be acquired in various ways, but the most common method currently is with the use of a charge coupled device (CCD) video camera interfaced to a PC in order to acquire 'frames' of diffraction patterns.

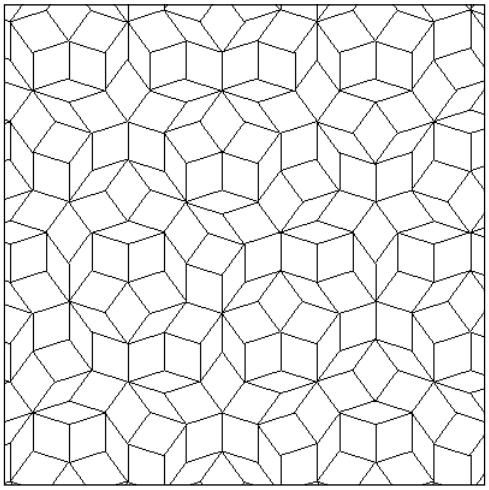

Figure 1. A Penrose tiling (from figure 2 of [1]).

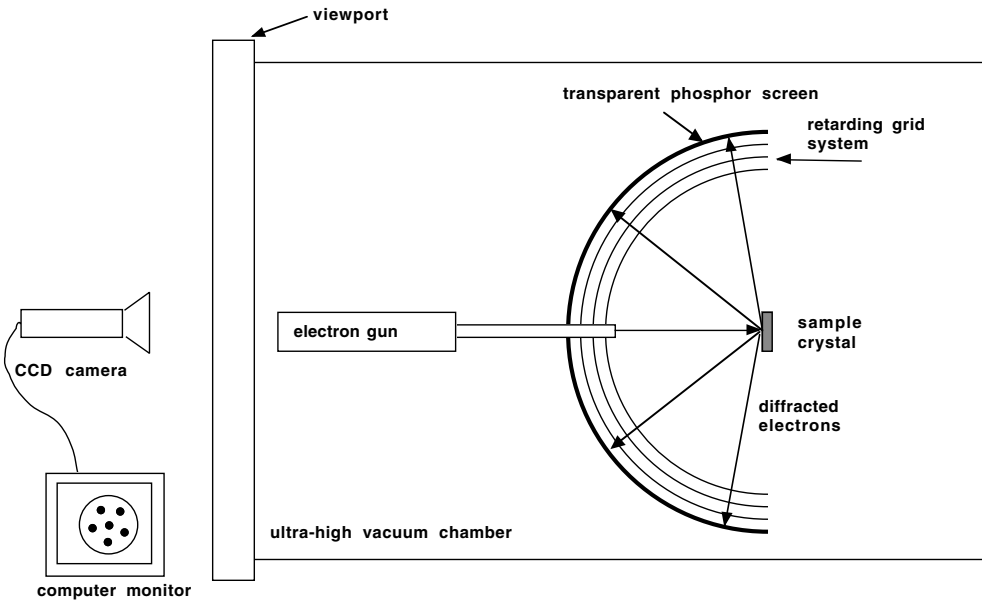

Figure 2. Schematic diagram of a typical LEED experiment. The electron gun produces the monoenergetic electron beam, the hemispherical grid system repels the electrons having energies below the elastic energy and the diffracted electrons are then accelerated toward the phosphor screen where they produce the LEED pattern. The LEED pattern can be viewed through the viewport, and data may be recorded with a CCD camera.

2.2. Ewald construction and the reciprocal lattice

LEED from periodic surfaces has generally been described in terms of an Ewald sphere construction [4], as shown in figure 3. In the simplest case, the reciprocal lattice of a surface comprises periodically spaced rods that run perpendicular to the surface plane (figure 3(a)). The Ewald sphere (figure 3(b)) has a radius equal to the magnitude of the wavevector of the

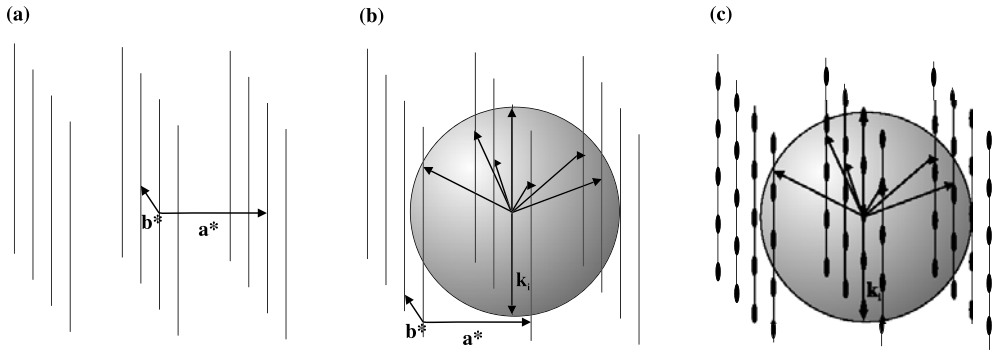

Figure 3. (a) Reciprocal lattice rods for a two-dimensional periodic lattice. The reciprocal lattice unit cell vectors are denoted as a^* and b^*. (b) Ewald sphere construction. The incident wavevector is denoted as k_i. All possible diffraction peaks for this incident wavevector are located at the intersection of the diffraction rods and the Ewald sphere. (c) Ewald construction showing the locations of the intensity variations along the rods due to the 3D periodicity of the lattice.

diffracting electrons, and is generally drawn such that the end of the incident wavevector intersects the origin of reciprocal space. The intersections of all other parts of the sphere with the reciprocal lattice rods provide the positions of all possible diffraction peaks from the surface structure that generates this set of rods. By varying the magnitude of the wavevector, it is possible to measure the intensities along the rods. For a perfect two-dimensional structure, this intensity will be constant along each rod, but the 3D character of any surface will introduce variations in the intensity measured along the rods, as depicted in figure 3(c). It is precisely this intensity variation that provides the most detailed information about the surface geometry.

If the surface is a truncation of the bulk structure, then in the kinematic (single-scattering) approximation the highest intensities will be observed at the locations of the 3D reciprocal lattice points. These points represent the Bragg conditions, where the scattering from the entire 3D lattice is in phase. In most situations, however, the surface is not a simple truncation of the bulk structure, and the intensities along the rods are more complicated than a straightforward projection of the bulk diffraction pattern. When interpreting the measured intensities along the rods in a LEED experiment, one must additionally consider the effect of multiple scattering (where the electron wave is scattered by more than one reciprocal lattice vector), which can cause a considerable difference between the actual measured intensities and those predicted by a simple structure factor calculation. The damping of the electron wave at the surface and thermal effects also produce significant changes to the measured intensities.

The intensity profiles of the diffraction spots, or scans across the rods (often called ω scans in x-ray diffraction terminology), are often used to obtain information about the degree of surface order [5]. The simplest, and perhaps the most common, type of defect on a well prepared surface is a step separating two terraces of different heights. The effect of random, up-and-down, single-atomic-height steps on the diffraction rods is to broaden them periodically, leading to wider diffraction peaks at certain scattering conditions [5]. When the scattering from all surface terraces is in phase (in the absence of surface relaxation, this will be at the 3D Bragg points) the steps effectively will be invisible, and the diffraction peaks will be as narrow as from a perfect surface. An Ewald construction showing this effect is shown in figure 4. The degree of broadening of the rod (and hence the diffraction peak) is a measure of the average terrace width on the surface, and the distance between in-phase scattering conditions is a measure of the step height. It should be noted that this technique may be used to determine the average step height (i.e. the distance between the top two planes) whether or not this distance is the

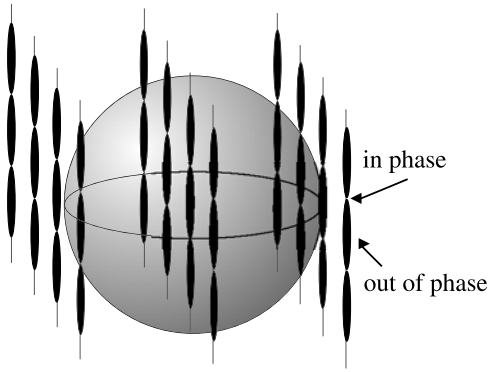

Figure 4. Ewald sphere construction showing the reciprocal lattice rods from a surface that has random single-height steps. At the out-of-phase conditions, the rods are broadened by an amount that is inversely related to the average terrace width. The distance between successive in-phase conditions is related inversely to the average step height.

same as the bulk interplanar spacing, since the broadening described here arises solely from the finite lateral extent of the terraces.

2.3. Dynamical LEED

In order to obtain more detailed information about the surface geometry, it is usually necessary to compare the measured integrated (across the rods) intensities as a function of distance (in momentum space) along the rod to calculated intensities from model structures. In a typical experiment, diffraction 'frames' are acquired at closely spaced energies (e.g. 1 eV) over a wide energy range (e.g. 50–500 eV). The intensities of different diffraction beams are then extracted and plotted as a function of energy. The intensities of different but symmetrically equivalent diffraction spots may be averaged in order to reduce noise and the effect of minor experimental misalignment. These experimental curves are then compared to calculated curves using a reliability factor (*R*-factor) to provide a quantitative measure of the level of agreement.

The model calculations for a dynamical LEED analysis are typically carried out using one of the several programs that have been written for this purpose. The most widely used program is probably the tensor LEED program, developed by many LEED practitioners and available for download from http://electron.lbl.gov/vanhove/[6], although other programs exist, each having a somewhat different approach or emphasis. All include a representation of the scattering potential of the atoms, a representation of the surface geometry, a method for the calculation of the effect of multiple scattering on the intensities and thermal and damping effects.

2.4. Symmetry effects in LEED patterns from periodic structures

Just as the diffraction pattern from a linear grating is symmetric about the origin, the diffraction pattern from a two-dimensional grating is also symmetric about the origin. Thus, the diffraction pattern from a two-dimensional grating having twofold symmetry has twofold symmetry, the diffraction pattern from a grating having fourfold symmetry has fourfold symmetry, but the diffraction pattern from a grating having threefold symmetry has sixfold symmetry. In other words, the diffraction pattern from any two-dimensional grating will possess inversion symmetry about its origin.

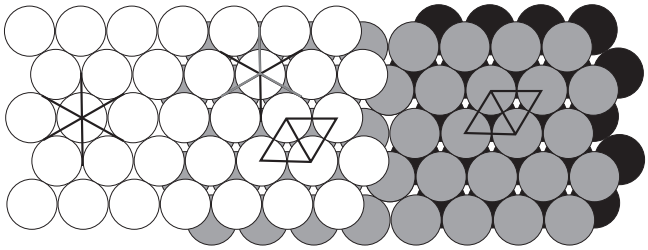

Figure 5. The atomic structure of an hcp (001) surface. On the left, a single layer is shown. This layer has a sixfold rotational symmetry axis, as shown. In the centre, two layers of the surface are shown. Here, the sixfold symmetry has been broken, and the overall symmetry is threefold in terms of a LEED experiment, because the top-layer and second-layer atoms are not equivalent in terms of the phase change (and amplitude) produced in the scattered wave. A threefold rotation axis is shown in the central part of the diagram. If the central part of this diagram is considered to be an 'A' termination of the hcp surface, the right-hand side shows two layers of a 'B' termination. By examining the structure within the unit cells (parallelograms) of these surfaces, it is evident that they are not identical, but that they are related by a mirror reflection through a plane that cuts the unit cell in half.

The diffraction from real surfaces differs from diffraction from two-dimensional arrays in several ways. Additional phase shifts are introduced in the diffraction from surfaces by the scattering from atoms that are not co-planar (including those in deeper layers) and also by different atom types. In order to illustrate these effects, we take here the example of the diffraction from a surface with hexagonal symmetry. The top layer of a single-element hexagonal-close-packed (hcp)(001) surface has sixfold symmetry, as shown in figure 5. The diffraction pattern from this layer will also be sixfold. However, the LEED pattern from a perfect hcp(001) surface is threefold because electrons scatter not just from the top layer, but from deeper layers. Figure 5 shows that for the top two layers of this surface the overall symmetry is threefold. Because there is a phase difference in the waves scattering from the two different layers, the conditions for constructive interference will generally display threefold symmetry.

A perfectly terminated hcp(001) surface indeed produces a LEED pattern with threefold rather than sixfold symmetry. However, it is more common to observe a sixfold symmetric LEED pattern from hcp(001) surfaces. This is due to surface defects, in particular to surface steps that cause different surface terminations to coexist. An hcp(001) surface that comprises equal numbers of A and B terminations produces a LEED pattern with sixfold symmetry, because the two terminations are related to each other by a mirror reflection, as illustrated in figure 5. We note for completeness that this mirror reflection symmetry is not present in the different terminations of an fcc(111) surface. In that case, all terminations (A, B and C) are identical, and therefore the LEED pattern is always observed to have threefold symmetry.

3. Low-energy electron diffraction from quasicrystals

3.1. Diffraction from a Fibonacci array

The effect of quasicrystallinity on a diffraction pattern is most readily seen in the Fourier transform of a Fibonacci array, which is an example of one-dimensional aperiodic order. A Fibonacci array is a linear sequence of two elements, one long and one short, and is defined by a set of rules that governs its generation. These rules are that each successive sequence is generated from the previous one by replacing each short element by a long one, and each

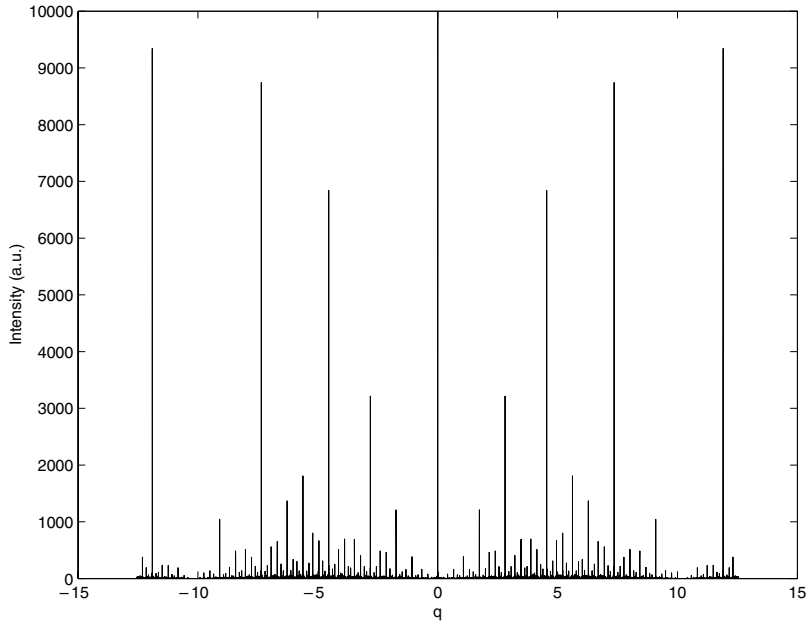

Figure 6. Fourier transform of a 10 000-component Fibonacci sequence. The scale of q is set by the short length segment of the Fibonacci sequence, i.e. $q = 1$ corresponds to the inverse length of the short segment of the Fibonacci sequence.

long element by a long one and a short one. How these rules generate a Fibonacci array is illustrated here:

S
L
LS
LSL
LSLLS
LSLLSLSL
LSLLSLSLLSLLS
LSLLSLSLLSLLSLSLLSLSL
LSLLSLSLLSLLSLSLLSLSLLSLLSLSLLSLLS

The Fourier transform of a typical sequence from this array is comprised of densely spaced sharp peaks, as shown in figure 6. Although there is an infinite number of peaks, only a certain fraction of these have appreciable intensity. The intensity is symmetric about the origin, but the spacing of the most prominent peaks is not periodic. These features have also been observed in the patterns generated by the diffraction of laser light through gratings that have lines in a Fibonacci array [7]. The diffraction from a two-dimensional quasicrystalline array will have similar properties, extended over two dimensions. This can be seen in the laser diffraction pattern from a grating having fivefold rotational symmetry, as shown in figure 7. The diffraction pattern is symmetric about the origin, having tenfold (not fivefold) symmetry, with aperiodic prominent peaks.

Initially, the most surprising aspect of the diffraction from a quasicrystal is the presence of sharp peaks, given the lack of periodicity in the structure. The presence of densely spaced, sharp diffraction peaks from quasicrystalline order has been described before in terms of the structure being comprised of two or more mutually incommensurate lattices [8–10]. Considering a

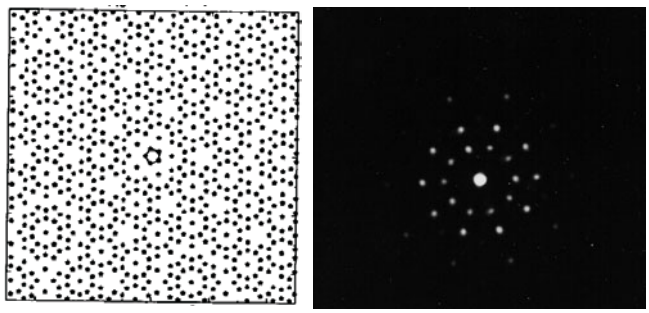

Figure 7. A two-dimensional structure having fivefold rotational symmetry and the tenfold diffraction pattern obtained using this structure as a grating in front of a laser.

one-dimensional quasicrystal, the positional order of atoms can be described as a sum of two functions, each of which is periodic, but with mutually incommensurate periods [8, 10]. If only one of these functions were present, the diffraction pattern would consist of peaks spaced periodically in reciprocal space with spacing k_1. The second term alone would give periodically spaced peaks in reciprocal space with spacing k_2. Because the two periods are incommensurate (i.e. their periods are irrational multiples of each other), the full diffraction pattern will consist of all of the peaks produced by each period alone, plus peaks at all linear combinations of k_1 and k_2. In two or three dimensions, the peaks will be densely spaced in two or three dimensions, respectively, with the added rotational symmetry that reflects the bond-orientational order present in the quasicrystalline structure [9, 10].

3.2. LEED from quasicrystal surfaces

Because of their novelty, much of the interest in quasicrystal surfaces has focused on those surfaces that have fivefold or tenfold symmetry. The surfaces most often studied, and which will be described in this paper in more detail later, are the fivefold surface of icosahedral Al–Pd–Mn and the tenfold surface of decagonal Al–Ni–Co. As described elsewhere in more detail [1, 11, 12], icosahedral quasicrystals are aperiodic in every direction, whereas the decagonal quasicrystals are periodic in the direction parallel to the tenfold symmetry axis. These properties themselves lead to some interesting effects in the diffraction patterns obtained from these surfaces.

It is observed that the fivefold surface of icosahedral Al–Pd–Mn produces a fivefold symmetric LEED pattern [13], while the tenfold surface of decagonal Al–Ni–Co produces a tenfold symmetric LEED pattern [14], as shown in figure 8. As described earlier for the case of two-dimensional periodic arrays, the diffraction from a purely two-dimensional array of identical atoms having either fivefold or tenfold rotational symmetry would produce a tenfold symmetric diffraction pattern. However, the presence of different atom types, the non-coplanar arrangements of atoms and the partially attenuated scattering from the deeper layers will generally break that tenfold symmetry, giving a fivefold LEED pattern.

This raises the question of why the LEED pattern from decagonal Al–Ni–Co is observed to be tenfold. This is a particularly interesting question in view of the bulk model structures for Al–Ni–Co, which indicate that individual planes of Al–Ni–Co may actually have fivefold rotational symmetry, and the overall tenfold decagonal symmetry is achieved by a tenfold screw axis, i.e. each plane is related to its neighbouring planes by a $\pi/5$ rotation and a translation perpendicular to the plane [15]. Therefore, a perfectly terminated surface would have fivefold

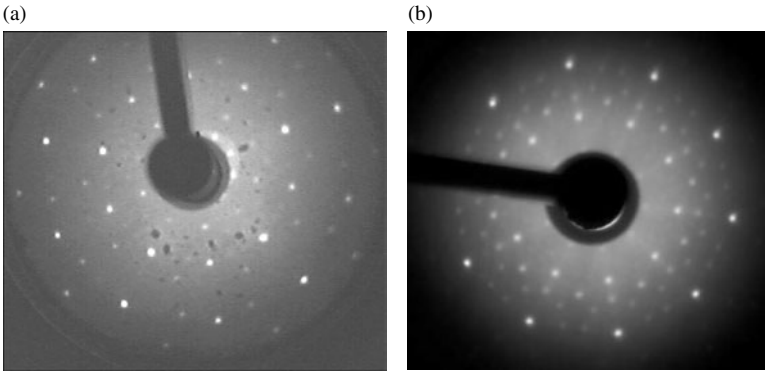

Figure 8. LEED patterns from (a) icosahedral Al–Pd–Mn (66 eV) and (b) decagonal Al–Ni–Co (72 eV).

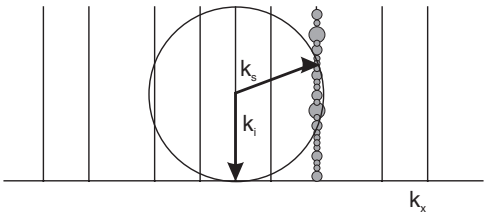

Figure 9. A two-dimensional cut through an Ewald sphere construction for a quasicrystal. For one reciprocal lattice rod, hypothetical 3D Bragg points are indicated by circles of various diameters, denoting peaks having different intensities (not different widths).

symmetry. In analogy with the case of the hcp(001) surface described earlier, the observation of a tenfold symmetric LEED pattern indicates that more than one surface termination is present, and that the different surface terminations are related to each other by a (mirror or rotation) symmetry operation. The decagonal structure of Al–Ni–Co is quasiperiodic within the tenfold planes, but periodic in the direction perpendicular to these planes. For the tenfold surface of Al–Ni–Co, the layer stacking sequence is believed to be ABAB [15, 16]. If this is the case, the tenfold symmetry of the LEED pattern indicates that the two terminations are present at the surface in equal amounts and are related to each other by a mirror or rotation symmetry operation. It is also strongly suggestive of a surface composed of terraces separated by single-height steps, which is consistent with STM observations of this surface [17].

In summary, the observed LEED pattern from a perfect quasicrystal surface (i.e. no defects) that has fivefold symmetry or tenfold symmetry will generally have fivefold symmetry. If tenfold symmetry is observed, this is an indication that equal numbers of different terminations, related by a mirror or rotational symmetry, are present. (It is possible to envision a tenfold surface where the symmetry is not broken by the stacking sequence, e.g. if the stacking is AAAA, or by non-co-planar or different atom types, but this is an extremely unlikely scenario.)

3.3. LEED intensity measurements from quasicrystal surfaces

Figure 9 shows a two-dimensional cut through an Ewald sphere construction for a hypothetical perfect fivefold or tenfold quasicrystal surface, showing just the rods that have the highest intensities. The rods are arranged aperiodically, similar to the Fourier transform of the one-

dimensional Fibonacci sequence. In general, there will be non-zero intensity at an infinite number of points along each of the rods, in the same sense as observed in the Fourier transform of the Fibonacci array (figure 6). Since some small fraction of these have higher intensities than the rest, the measured intensities will vary if one scans along the rods, as in a LEED $I(E)$ experiment. If the surface is a simple truncation of the bulk structure, the intensities along the rods will peak at the positions of the highest-intensity 3D diffraction points. In general, these positions will also be aperiodic, although in the special case of the tenfold surface of a decagonal quasicrystal they will be periodic.

As noted in the previous section, the intensity profiles of the diffraction rods can give information about surface defects such as steps. For the case of a tenfold decagonal quasicrystal surface, which has periodically stacked planes and one predominant step height, there are clear conditions for in-phase and out-of-phase scattering, as demonstrated by the measurements in the next section. In the case of the icosahedral surfaces, the situation is more complicated. In principle, every point along a diffraction rod is a 3D Bragg point, and one might expect no variation in the widths of the diffraction profiles. Using LEED, however, only a few layers at the surface are sampled, and this, along with surface relaxation and the possibility that not all possible planes are likely to be surface terminations, may allow out-of-phase scattering to be observed. Such a study for fivefold Al–Pd–Mn is presented later in this paper.

To obtain more details about the surface geometry, a dynamical LEED analysis can be used. The formalism for dynamical LEED and most of the available analysis programs, including the tensor LEED program mentioned earlier, were originally developed for periodic structures having a well defined atomic geometry within a repeating unit cell. Quasicrystal surfaces therefore present a special challenge for the computational part of a dynamical LEED study. The approach that has been developed thus far to deal with quasicrystal surfaces uses a combination of exact calculation and approximation, and is described later in this paper.

4. Tenfold surface of decagonal Al–Ni–Co—a spot profile analysis

As discussed above, the positions along the rods of the dominant diffraction intensities will, in general, be aperiodic. However, the order perpendicular to the tenfold direction of a decagonal quasicrystal is periodic. That periodicity should give rise, in the kinematic approximation, to periodic in-phase scattering conditions along the rods.

Gierer *et al* [14] studied the tenfold surface of decagonal Al–Ni–Co using spot-profile-analysis LEED (SPA-LEED). Earlier studies of the bulk structure using x-ray diffraction and transmission electron microscropy had determined that the bulk structure of Al–Ni–Co consists of periodic planes separated by an average interlayer distance of 2.04 Å [15, 16, 18–21]. The period of the stacking sequence was found to depend on the exact composition, but all of the bulk structural determinations have found a structure that has essentially an ABAB stacking. In the Ni-rich structure, all planes are exactly the same (and related by a symmetry operation), whereas slight structural differences in planes are observed in the Co-rich structures that lead to a stacking sequence denoted by some authors by ABA′B′, where the differences between the primed and unprimed layers are rather subtle and include the degree of planarity of the layers and/or interlayer spacings. The purpose of the LEED study was to elucidate the structure of the surface region.

As described above, the interplanar spacing in a decagonal quasicrystal can be obtained if one can identify the locations of successive in-phase conditions along the diffraction rods. On a perfectly truncated quasicrystal, one would need to rely on measuring the intensities along the rods. However, a precise determination for just the top interlayer spacing can be made by measuring the widths of the diffraction peaks along the rods, as long as there are

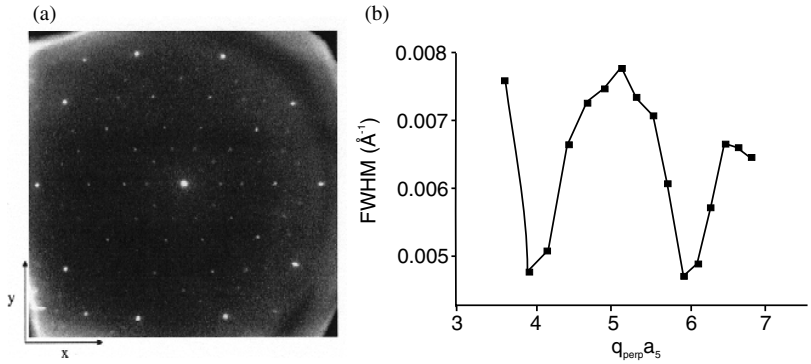

Figure 10. (a) SPA-LEED pattern from Al–Ni–Co at 60 eV. (b) FWHM of the specular diffraction peak as a function of the perpendicular momentum transfer, multiplied by 4.08 Å$/2\pi$ [13].

some surface defects that give rise to a broadening of the diffraction profiles at the out-of-phase conditions. Such measurements require surface defects having an average range that is less than the transfer width of the instrument, and this makes SPA-LEED instruments, which typically have transfer widths greater than 1000 Å (compared to about 100 Å for conventional LEED apparatus) appropriate [22].

Figure 10(a) shows an observed diffraction pattern, and figure 10(b) shows the measured width of the specular diffraction peak from Al–Ni–Co as a function of the perpendicular momentum transfer (multiplied by 4.08 Å$/2\pi$). The condition for in-phase scattering from successive terraces is

$$q * d = 2\pi n,$$

where q is the perpendicular momentum transfer, d is the step height and n is an integer. Therefore for single-height steps, the diffraction peak width should have minima where $q * d/2\pi$ is equal to an integer. It can be seen from the graph that minima occur only near even integers when d is set to 4.08 Å, and therefore the step height is about half that. The analysis of these data indicates a step height of 2.05 ± 0.05 Å, which is consistent with the measured bulk interlayer distance of 2.04 Å.

The measurement of the full width at half maximum (FWHM) of the diffraction peaks at their out-of-phase conditions allows the determination of the average terrace length $\langle L \rangle$. After deconvolution with the in-phase profile, the average terrace width in this case was found to be 170 Å. The peak widths at the in-phase scattering condition corresponded to a length of 200 Å, much smaller than the instrumental width, indicating that the surface region was not entirely homogeneous, perhaps due to phason disorder or strain.

Therefore, simply by measuring the peak widths as a function of the beam energy (or equivalently, along the diffraction rods), it was possible to determine that the tenfold surface of Al–Ni–Co prepared in this way has essentially an unrelaxed truncated-bulk structure and an average terrace width of about 170 Å. This method could be employed, if the quality of the sample were sufficient, to measure the surface morphology as a function of surface preparation parameters, such as sputtering and annealing temperature and times.

5. Fivefold surface of icosahedral Al–Pd–Mn—a spot profile analysis

A similar analysis of data from an icosahedral quasicrystal would not be necessarily expected to provide similar information on interlayer spacings because the icosahedral quasicrystals

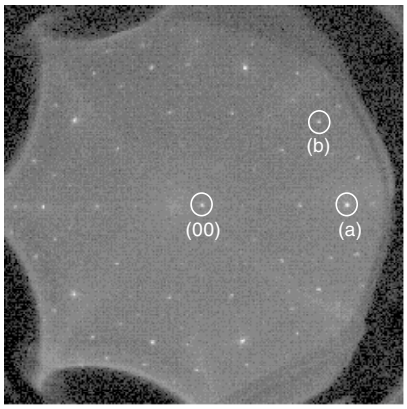

Figure 11. SPA-LEED pattern for Al–Pd–Mn at 70 eV. The diffraction spots used in this study were the specular (00) spot and the two spots labelled (a) and (b).

are not periodic in any direction. Because there are an infinite number of 'Bragg points' in the 3D reciprocal lattice [8], one might expect no variation in the diffraction peak widths for icosahedral quasicrystals. However, if the surface of the quasicrystal is dominated by one type of surface termination, then it is possible that one prominent interlayer spacing will give rise to oscillations in peak width similar to those observed for the decagonal quasicrystal. In order to explore this further, an experiment, similar to that described above for Al–Ni–Co, was carried out by us on the fivefold surface of Al–Pd–Mn. These data are not published elsewhere, and therefore the procedures used will be described more fully.

The Al–Pd–Mn quasicrystal sample was provided by Ames Laboratory and was cut and polished using techniques described before [23]. The surface was prepared in ultra-high vacuum by argon ion bombardment followed by annealing the surface to 970 K for several hours. The surface cleanliness was checked before each set of LEED experiments using Auger electron spectroscopy, and in general the level of impurities was below detectability. The SPA-LEED instrument used in this study had a measured transfer width of approximately 1100 Å, and the lateral momentum transfer scale was calibrated using a Pt(111) crystal and its known lattice constant.

The two-dimensional diffraction pattern at 70 eV is shown in figure 11. Diffraction peak profiles were measured for the specular beam and for the two diffraction peaks labelled in the LEED pattern. While the spots in this pattern appear to be very sharp, at higher resolution it is evident that the diffraction beams are typically composed of several peaks. This was an indication that the sample is not a perfect single grain: that there are defects such as multiple phases, phason disorder or strain-induced disorder present. However, in many cases where the peaks were resolved, the peak widths can often be measured to have essentially the instrumental width, indicating that several relatively large ($\gg$1000 Å) single-grain areas are present in the area of the SPA-LEED beam, which is about 1 mm across.

In order to analyse the peak profiles, the peaks were fitted to Lorentzian lineshapes, and where necessary multiple Lorentzian lineshapes were convolved to fit the profiles. The Lorentzian peak width was an adjustable fitting parameter. Figure 12(a) shows the width (FWHM) of the specular peak as a function of the perpendicular momentum transfer. Compared to the earlier study of Al–Ni–Co, the diffraction peaks are narrower, ranging from close to the instrumental width (about 0.001) to 0.004 Å^{-1}. The narrower peaks indicate that the underlying quasicrystalline structure is more perfect in this sample than in the one used in the earlier Al–Ni–Co study.

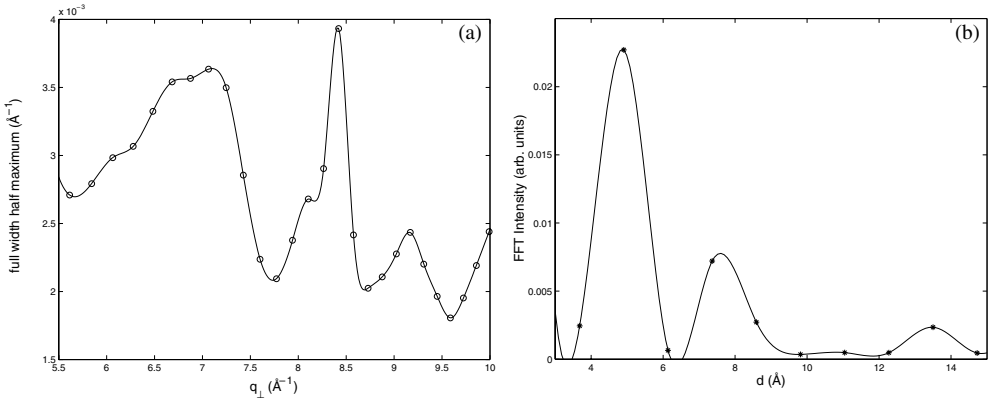

Figure 12. (a) FWHM for the specular peak from Al–Pd–Mn versus q-perpendicular. These data points represent the fitted widths of the Lorentzian fits, and the curve is a spline-interpolated polynomial fit. (b) Intensity of the fast Fourier transform harmonics as a function of step height.

Because there are, in principle, a large number of surface terminations and a large number of possible step heights, it is not possible to use the same analysis technique as in the Al–Ni–Co study. However, earlier STM studies have suggested that there are just two or three dominant step heights present on the fivefold surface of Al–Pd–Mn [24, 25], and this makes a Fourier transform analysis feasible. Figure 12(b) shows the fast Fourier transform of the data shown in figure 12(a). The major peaks in this spectrum occur at about 4.4 and 7 Å, with estimated errors of about ± 1 Å. It is not possible from these data to explore peaks corresponding to smaller step heights because the energy range of measurable LEED intensities is short (30–150 eV). This fact also produces the large uncertainty in the step height determination. Nevertheless, the values obtained agree with the two primary step heights measured in the earlier STM studies [24, 25]. Similar measurements were carried out for two additional diffraction spots, for profiles taken in two perpendicular directions for each, resulting in average step height values of 4.4 ± 0.3 and 7.2 ± 0.5 Å. These values are comparable to the step heights determined by the STM studies of 4.1 and 6.4 Å [24, 25]. This experiment demonstrates that, even in the case of non-periodic layer stacking, it is possible to extract step heights using a relatively simple LEED analysis.

6. Dynamical LEED study of icosahedral Al–Pd–Mn—a LEED $I(E)$ analysis

The approach described in the previous sections provides a method for the determination of the average step heights at the surface, and therefore provides information about some average interlayer spacings and also the degree of lateral order in the quasicrystal surface, but it does not provide information on the surface geometries. In a quasicrystal surface, as in the bulk, there are a large number of local geometries present. This presents a challenge both for the determination of the atomic-scale surface structure and for its description. A dynamical LEED analysis helps to meet this challenge, and such an experiment for the fivefold surface of Al–Pd–Mn is described here [13, 26, 27].

Like the experiments described above, a dynamical LEED experiment requires the measurement of the intensities of the diffracted beams as a function of the incident electron energy. The difference is that in a dynamical LEED analysis one must calculate the scattered intensities (including multiple scattering) from model structures in order to obtain the detailed surface structure. The formalism for LEED was originally developed for periodic structures

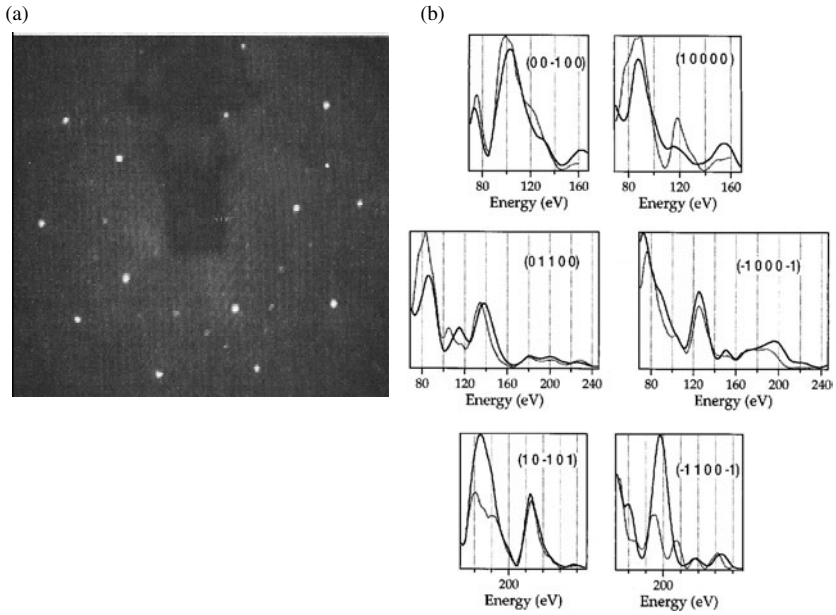

Figure 13. (a) LEED pattern and (b) $I(E)$ curves for Al–Pd–Mn [26].

having a well defined atomic geometry within a repeating unit cell [28]. While the advances in computing power have supported the studies of structures with larger and larger unit cells [29], the lack of a finite unit cell at quasicrystal surfaces presents a special challenge for the computational part of a dynamical LEED study.

The diffraction pattern and the LEED $I(E)$ curves obtained from the Al–Pd–Mn dynamical LEED experiment are shown in figure 13 [26]. To deal with the large number of different atom types (i.e. different local environments) that must be considered in the model calculation, approximation techniques are necessary, and several different approximation techniques were implemented in this work [13, 26].

The model structures used in this study were based on the bulk structure determined by x-ray and neutron diffraction [30]. From this bulk structure, a large number of possible bulk-like surface terminations were generated. In order to reduce the number of atoms in the model with different scattering properties, each plane was characterized in terms of its atomic composition and density. An artificial atom having average scattering properties was then generated for each plane using the average t-matrix approximation [31–33]. For the multiple scattering, an approximation called the 'average neighbourhood approximation' was used, in which the variable local environments of atoms in any particular plane were replaced by a fixed, simplified average geometry. Within this approach, the average neighbourhood of an atom is described by a distribution function in which the number of neighbour atoms is distributed uniformly on rings, with the proper polar angles but without regard to azimuthal angles. This method was further refined by separating the planes into subplanes, each containing only atoms of similar local environment. This procedure was employed to make more accurate the assumption that the scattering properties of all atoms within a subplane are equal. Within this approach, the $I(E)$ curves could be calculated for a quasicrystal with a small number of atoms with different scattering properties, typically about 10.

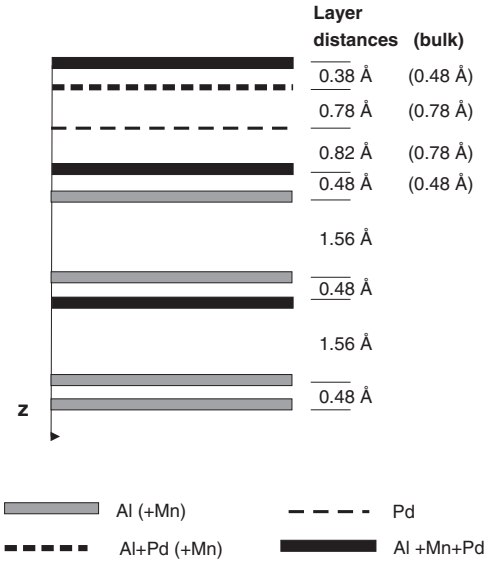

Figure 14. Optimum termination determined by dynamical LEED study [26]. The first four layer spacings were optimized (the corresponding bulk values are shown in parentheses). Deeper interlayer spacings were kept fixed at their bulk values. The planes are drawn at their respective depths z, as bars with thickness proportional to the atomic density in each plane, together with their approximate composition, as labelled below.

In the comparison of the experimental and calculated LEED spectra, it was first assumed that the surface had a single termination of the bulk structure, and the top two planes were relaxed to produce the best agreement. Of all of the terminations tried, it was found that better agreement was obtained for terminations that contained a pair of closely spaced dense layers, the top layer being primarily Al, and the bottom one being a mixture of Al and Pd. In order to take into account the presence of different terminations, the ten terminations that produced the best agreement with the experimental spectra were averaged together. The optimum geometry obtained from this analysis is shown in figure 14. The topmost plane is relaxed inwards by 0.06 ± 0.04 Å relative to the bulk planes, while the deeper planes are essentially in their bulk positions. The distance between the first and second planes is contracted by about 0.1 Å relative to the bulk value of 0.48 Å. The average chemical composition of the topmost atomic planes is 93% Al and 7% Mn for the topmost plane, and 49% Al, 42% Pd and 9% Mn for the second plane. The averaged lateral density of the two topmost planes taken together is 0.136 atoms Å^{-2}, comparable to that of a single plane of Al(111) (0.141 atoms Å^{-2}).

In this first dynamical LEED study of a quasicrystal surface, even though the exact atomic geometries were not obtained, it was possible to obtain a significant amount of information about the surface structure. A second similar study by the same group for another icosahedral quasicrystal, Al–Cu–Fe [34], produced both a similar result and similar level of agreement between the experimental data and the model calculations. That surface also was found to be essentially bulk terminated, with a contraction of the top layer relative to the bulk. The preferred terminations were found to have similar atomic densities and chemical compositions to those on Al–Pd–Mn.

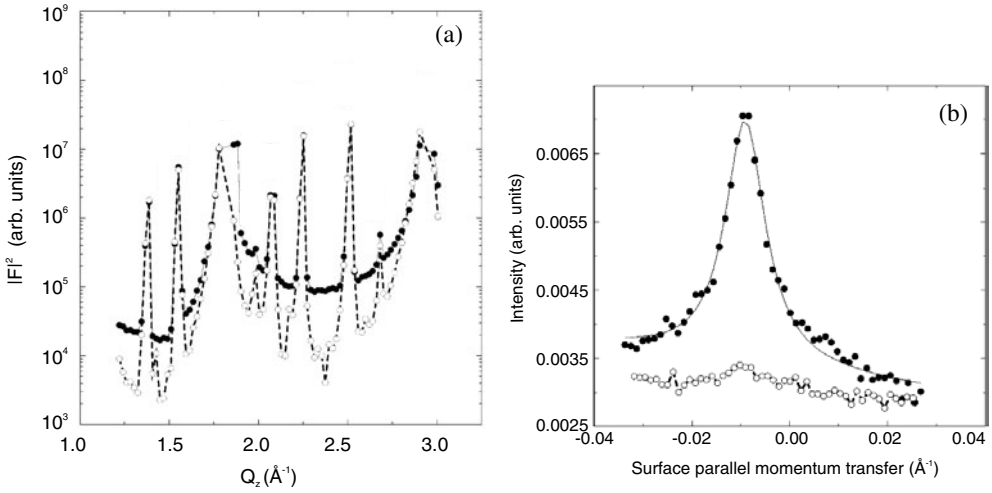

Figure 15. (a) Specular crystal truncation rod perpendicular to the fivefold i-Al–Pd–Mn quasicrystal surface after annealing (filled circles) and ion sputtering (open circles) [35]. The narrow peaks are bulk Bragg peaks. (b) Transverse scan at a minimum between Bragg peaks. Filled circles correspond to the annealed sample and open circles correspond to the same sample after ion bombardment.

7. Other surface diffraction techniques

While most of the diffraction studies of quasicrystal surfaces have used LEED, other diffraction probes can provide complementary information about these surfaces. Two other diffraction techniques that already have been applied to quasicrystal surfaces are surface x-ray diffraction and He-atom diffraction. X-ray diffraction provides similar information to that obtained in a LEED experiment, but in principle has a simpler analysis procedure since multiple diffraction events do not occur. He-atom diffraction is a truly surface-sensitive technique since the He atoms do not penetrate the surface. Hence, it offers a better means of studying the overall symmetry of the outer layer of atoms at the quasicrystal surface. For completeness, these two studies are described here.

7.1. Surface x-ray diffraction

Surface x-ray diffraction has been applied to study the fivefold surface of Al–Pd–Mn [35]. In this study, a truncation rod analysis was used to obtain information about the terminating surface layer. Essentially, this type of experiment is analogous to a LEED $I(E)$ experiment where the diffraction intensities along the reciprocal lattice rods are measured. In this experiment, just the specular rod was considered, which has higher symmetry than the other rods and thus allows a simpler analysis to be performed.

Figure 15(a) shows the measured specular rod intensity as a function of perpendicular momentum transfer for both a sputtered surface (open circles) and an annealed surface (closed circles). The peaks present in these spectra are the bulk Bragg peaks, and the underlying shape of the curve from the annealed sample represents the lineshape of an almost perfectly flat surface [35]. The decrease of intensity between the Bragg peaks of the spectrum from the sputtered sample provides an indication of the effect that surface defects has on this spectrum.

In other words, the more two dimensional (flatter) the sample, the more uniform the intensity is along the rods, whereas for a more three-dimensional surface (i.e. one having many defects), the lower the intensity between the sharp Bragg peaks, and the spectrum approaches that of the bulk solid (which would have intensity only at the 3D Bragg points).

Figure 15(b) shows two corresponding scans across the specular rod between Bragg peaks, the width of which gives a measure of the lateral domain width. The width of this rod indicates the average lateral domain width to be 380 Å for this sample. Further analysis of the rod intensities were achieved by performing structure factor calculations for model structures and comparing them to the measured intensities. The parameters that were varied in this analysis were the perpendicular position of the top layer and the atomic concentrations in that layer, i.e. the same parameters that were varied in the dynamical LEED analysis. The results indicate that the top layer is both Al rich and Pd rich with respect to the bulk, and contracted relative to the average bulk termination distance of 0.83 ± 0.03 Å. The surface contraction agrees well with the earlier LEED study described above, although the conclusions about the composition differ somewhat in that the LEED study indicated there is some small concentration of Mn in the top layer (up to 10%), whereas the x-ray diffraction study indicates that there is none. Without further analysis, it is difficult to assess how meaningful that difference is, since there is almost certainly a range of different terminations present at the surface over the length scale probed by both of these techniques.

As for the LEED studies, this first study of a quasicrystal surface structure using x-ray diffraction has only just begun to exploit the potential of the technique. Additional information on the lateral surface order resides in the other truncation rods, which were not considered in this study. Thermal effects are also easily accessible with x-ray diffraction, and temperature dependent studies would be a natural extension to those already carried out.

7.2. He-atom scattering

The surface of Al–Pd–Mn was also studied using He-atom diffraction [36]. As a technique sensitive to just the outermost surface layer, He-atom diffraction is an excellent tool for studying the nature of and the degree of surface order. In this study, a fivefold diffraction pattern consistent with quasicrystalline order was observed. In light of the discussion in section 3 of this paper, and knowing that He-atom scattering samples only the outer layer of the surface, the observation of a fivefold diffraction pattern is proof of fivefold symmetry in the outer layer, or in at least some of the terminating terraces on this surface. It also indicates that the outer layer is comprised of more than one atom type (having different scattering potentials), or the outer-layer atoms are not entirely co-planar, or both of these. An analysis of the angular dependence of the specular intensity indicated a terrace size of about 450 Å. An analysis of the diffracted intensities indicates that the surface is very flat, with the amplitude of the first (fivefold) Fourier coefficient of the scattering potential being just 1.9 pm.

Again, this technique has not yet been fully exploited to study quasicrystal surfaces. One of the strengths of He-atom scattering as a tool to study quasicrystal surfaces will be evident in adsorption studies. Because of its extreme surface sensitivity, it scatters only from the top layer, thus allowing the adsorbate structure to be ascertained without the concern that the spectrum is dominated by the substrate structure. This is also a natural technique for quantitatively studying the surface morphology as a function of surface treatments, such as sputtering or annealing. The application of inelastic He-atom scattering can also be a useful probe of the dynamical properties of these surfaces, e.g. in studies of the diffusion of atoms across a quasicrystalline surface, or studies of the phonon dispersion in a quasicrystalline structure.

8. Conclusion

The studies described here prove that diffraction as a tool is adaptable to the non-periodic structures of quasicrystals, and the few studies carried out so far have been successful in providing new and complementary information about the nature of their surfaces. LEED has been the dominant diffraction technique applied to these surfaces so far, and is likely to continue to be for some time since LEED is ubiquitous in surface science laboratories. However, it is clear that there is much scope for extending and improving the analysis procedures of LEED and of other surface diffraction techniques to study quasicrystalline structures, because so far, only the most basic information has been extracted from these diffraction studies. For example, the details of the lateral ordering within the layers has not yet been accessed by diffraction studies, although in principle this information is accessible, and would provide a very useful complement to the many imaging studies of these surfaces. The thermal behaviour of these surfaces has not yet been explored in any detail using diffraction techniques. There is also considerable potential for the application of other diffraction methods to these surfaces.

Other surface diffraction and interference-based probes such as surface extended x-ray absorption fine structure (SEXAFS), and the normal incidence x-ray standing wave technique (NIXSW), which has been applied to the bulk quasicrystal structure [37], could be and should be applied to quasicrystal surfaces in order to obtain new and complementary information on the surface structure and geometry. Both SEXAFS and NIXSW will probably become more applicable and important in the study of adsorbates on quasicrystalline surfaces. In the case of SEXAFS, the chemical specificity of the adsorbate atoms or molecules will allow the surface signal to be decoupled from the bulk signal. In the case of NIXSW, adsorption geometries are likely to be accessible. Photoelectron diffraction has already been applied to the surfaces of Al–Pd–Mn [38–40] to study the local order of the surface, but it has not been fully exploited to determine the details of local geometries. In this case also, the technique is likely to become more important in the study of the geometries of adsorbates on quasicrystal surfaces.

Acknowledgments

We would like to thank W Allison, S D Barrett, D Litvin and K Pussi for useful discussions. We also thank Y Prishchepa for useful advice and assistance with data analysis. The Al–Pd–Mn sample used in the spot-profile-analysis study presented here was provided by T A Lograsso and A R Ross. This research was supported by NSF (DMR-9819977 and DMR-0208520) and EPSRC (grant numbers GR/N18680 and GR/N25718).

References

[1] McGrath R, Ledieu J, Cox E J and Diehl R D 2002 *J. Phys.: Condens. Matter* **14** R119
[2] International Union of Crystallography 1992 Report of the Executive Committee for 1991 *Acta Crystallogr.* **48** 922
[3] Watson P R, Van Hove M A and Hermann K 1996 *NIST Surface Structure Database Version 2.0, NIST Standard Reference Data Program* (Gaithersburg, MD: National Institute of Standards and Technology)
[4] Clarke L J 1985 *Surface Crystallography* (Chichester: Wiley)
[5] Henzler M 1982 *Surf. Sci.* **11/12** 450
[6] Barbieri A and Van Hove M A private communication (http://electron.lbl.gov/leedpack/)
[7] Litvin S Y, Romberger A B and Litvin D B 1988 *Am. J. Phys.* **56** 72
[8] Janot C 1992 *Quasicrystals: a Primer* (Oxford: Clarendon)
[9] Levine D and Steinhardt P J 1984 *Phys. Rev. Lett.* **53** 2477
[10] Levine D and Steinhardt P J 1986 *Phys. Rev.* B **34** 596

[11] Goldman A I, Sordelet D J, Thiel P A and Dubois J M (ed) 1997 *New Horizons in Quasicrystals* (Singapore: World Scientific)
[12] Stephens P W and Goldman A I 1991 *Sci. Am.* **264** 24
[13] Gierer M, Van Hove M A, Goldman A I, Shen Z, Chang S-L, Jenks C J, Zhang C-M and Thiel P A 1997 *Phys. Rev. Lett.* **78** 467
[14] Gierer M, Mikkelsen A, Gräber M, Gille P and Moritz W 2000 *Surf. Sci. Lett.* **463** L654
[15] Cervellino A, Haibach T and Steurer W 2002 *Acta Crystallogr.* B **58** 8
[16] Steurer W, Haibach T, Zhang B, Kek S and Lück R 1993 *Acta Crystallogr.* B **49** 661
[17] Kishida M, Kamimura Y, Tamura R, Edagawa K, Takeuchi S, Sato T, Yokoyama Y, Guo J Q and Tsai A-P 2002 *Phys. Rev.* B **65** 94208
[18] Yamamoto A and Weber S 1997 *Phys. Rev. Lett.* **78** 4430
[19] Joseph D, Ritsch S and Beeli C 1997 *Phys. Rev.* B **55** 1997
[20] Ritsch S, Beeli C, Nissen H-U, Gödecke T, Scheffler M and Lück R 1998 *Phil. Mag. Lett.* **78** 67
[21] Takakura H, Yamamoto A and Tsai A-P 2001 *Acta Crystallogr.* A **57** 576
[22] Scheithauer U, Meyer G and Henzler M 1986 *Surf. Sci.* **178** 441
[23] Ledieu J, Munz A, Parker T, McGrath R, Diehl R D, Delaney D W and Lograsso T A 1999 *Surf. Sci.* **433–435** 666
[24] Schaub T M, Bürgler D E, Güntherodt H-J and Suck J B 1994 *Phys. Rev. Lett.* **73** 1255
[25] Shen Z, Pinhero P J, Lograsso T A, Delaney D W, Jenks C J and Thiel P A 1997 *Surf. Sci.* **385** L923
[26] Gierer M, Van Hove M A, Goldman A I, Shen Z, Chang S-L, Pinhero P J, Jenks C J, Anderegg J W, Zhang C-M and Thiel P A 1998 *Phys. Rev.* B **57** 7628
[27] Gierer M and Over H 1999 *Z. Kristallogr.* **214** 14
[28] Van Hove M A and Tong S Y 1979 *Surface Crystallography by LEED (Springer Series in Chemical Physics vol 2)* (Berlin: Springer)
[29] Van Hove M A, Weinberg W H and Chan C-M 1986 *Low-Energy Electron Diffraction: Experiment, Theory and Surface Structure Determination (Springer Series in Surface Science vol 6)* (Berlin: Springer)
[30] Boudard M, de Boussieu M, Janot C, Heger G, Beeli C, Nissen H-U, Vincent H, Ibberson R, Audier M and Dubois J M 1992 *J. Phys.: Condens. Matter* **4** 10149
[31] Rous P J 1991 *Surf. Sci.* **244** L137
[32] Jona F, Legg K O, Shih H D, Jepsen D W and Marcus P M 1978 *Phys. Rev. Lett.* **40** 1466
[33] Gauthier Y 1996 *Surf. Rev. Lett.* **3** 1663
[34] Cai T, Shi F, Shen Z, Gierer M, Goldman A I, Kramer M J, Jenks C J, Lograsso T, Delaney D, Thiel P A and Van Hove M A 2001 *Surf. Sci.* **495** 19
[35] Alvarez J, Calvayrac Y, Joulaud J L and Capitan M J 1999 *Surf. Sci.* **423** L251
[36] Barbier L, Le Floc'h D, Calvayrac Y and Gratias D 2002 *Phys. Rev. Lett.* **88** 85506
[37] Jach T, Zhang Y, Colella R, de Boussieu M, Boudard M, Goldman A I, Lograsso T A, Delaney D W and Kycia S 1999 *Phys. Rev. Lett.* **82** 2904
[38] Naumovic D, Aebi P, Schlapbach L, Beeli C, Lograsso T A and Delaney D W 1999 *Phys. Rev.* B **60** R16330
[39] Naumovic D, Aebi P, Schlapbach L and Beeli C 1997 *New Horizons in Quasicrystals: Research and Applications* ed A I Goldman, D J Sordelet, P A Thiel and J M Dubois (Ames, IA: World Scientific) p 86
[40] Naumovic D, Aebi P, Schlapbach L, Beeli C, Lograsso T A and Delaney D W 1998 *Proc. 6th Int. Conf. on Quasicrystals* ed S Takeuchi and T Fujiwara (Tokyo: World Scientific) p 749